

## Biodegradation resistant multilayers coated with gold nanoparticles. Towards tailor-made artificial extracellular matrix

Vladimir Z. Prokopovic, Anna S. Vikulina, David Sustr, Claus Duschl, and Dmitry V. Volodkin

*ACS Appl. Mater. Interfaces*, **Just Accepted Manuscript** • DOI: 10.1021/acsami.6b10095 • Publication Date (Web): 08 Sep 2016

Downloaded from <http://pubs.acs.org> on September 9, 2016

### Just Accepted

“Just Accepted” manuscripts have been peer-reviewed and accepted for publication. They are posted online prior to technical editing, formatting for publication and author proofing. The American Chemical Society provides “Just Accepted” as a free service to the research community to expedite the dissemination of scientific material as soon as possible after acceptance. “Just Accepted” manuscripts appear in full in PDF format accompanied by an HTML abstract. “Just Accepted” manuscripts have been fully peer reviewed, but should not be considered the official version of record. They are accessible to all readers and citable by the Digital Object Identifier (DOI®). “Just Accepted” is an optional service offered to authors. Therefore, the “Just Accepted” Web site may not include all articles that will be published in the journal. After a manuscript is technically edited and formatted, it will be removed from the “Just Accepted” Web site and published as an ASAP article. Note that technical editing may introduce minor changes to the manuscript text and/or graphics which could affect content, and all legal disclaimers and ethical guidelines that apply to the journal pertain. ACS cannot be held responsible for errors or consequences arising from the use of information contained in these “Just Accepted” manuscripts.

1  
2  
3  
4  
5  
6  
7 Biodegradation resistant multilayers coated with  
8  
9  
10  
11 gold nanoparticles. Towards tailor-made artificial  
12  
13  
14  
15  
16 extracellular matrix  
17  
18  
19  
20

21 *Vladimir Z. Prokopović,<sup>a,b</sup> ‡ Anna S. Vikulina,<sup>a,c</sup> ‡ David Sustr,<sup>a,b</sup> Claus Duschl<sup>a</sup> and Dmitry V.*

22  
23  
24 *Volodkin<sup>\*a,c</sup>*

25  
26  
27 <sup>a</sup> Fraunhofer Institute for Cell Therapy and Immunology, Am Mühlenberg 13, 14476 Potsdam-  
28  
29 Golm, Germany.

30  
31 <sup>b</sup> University of Potsdam, Institute for Biochemistry and Biology, Maulbeerallee 2, 14469  
32  
33  
34 Potsdam, Germany.

35  
36 <sup>c</sup> School of Science and Technology, Nottingham Trent University, Clifton Lane, Nottingham  
37  
38 NG11 8NS, United Kingdom. E-mail: [dmitry.volodkin@ntu.ac.uk](mailto:dmitry.volodkin@ntu.ac.uk).

39  
40  
41  
42  
43 **Keywords:** Hyaluronic acid, polylysine, diffusion, semipermeable, fluorescence recovery after  
44  
45 photobleaching, layer-by-layer, enzymatic degradation, cell adhesion  
46  
47

48  
49  
50 **Abstract:** Polymer multicomponent coatings such as multilayers mimic extracellular matrix  
51  
52 (ECM) that attracts significant attention for their use as functional supports for advanced cell  
53  
54 culture and tissue engineering. Herein, biodegradation and molecular transport in  
55  
56 hyaluronan/polylysine multilayers coated with gold nanoparticles was described. Nanoparticle  
57  
58  
59  
60

1  
2  
3 coating acts as semipermeable barrier that governs molecular transport into/from the multilayers  
4 and makes them biodegradation resistant. Model protein lysozyme (mimics of ECM soluble  
5 signals) diffuses in the multilayers as fast and slow diffusing populations existing in an  
6 equilibrium. Such composite system may have high potential to be exploited as degradation-  
7 resistant drug delivery platforms suitable for cell-based applications.  
8  
9  
10  
11  
12  
13  
14  
15  
16

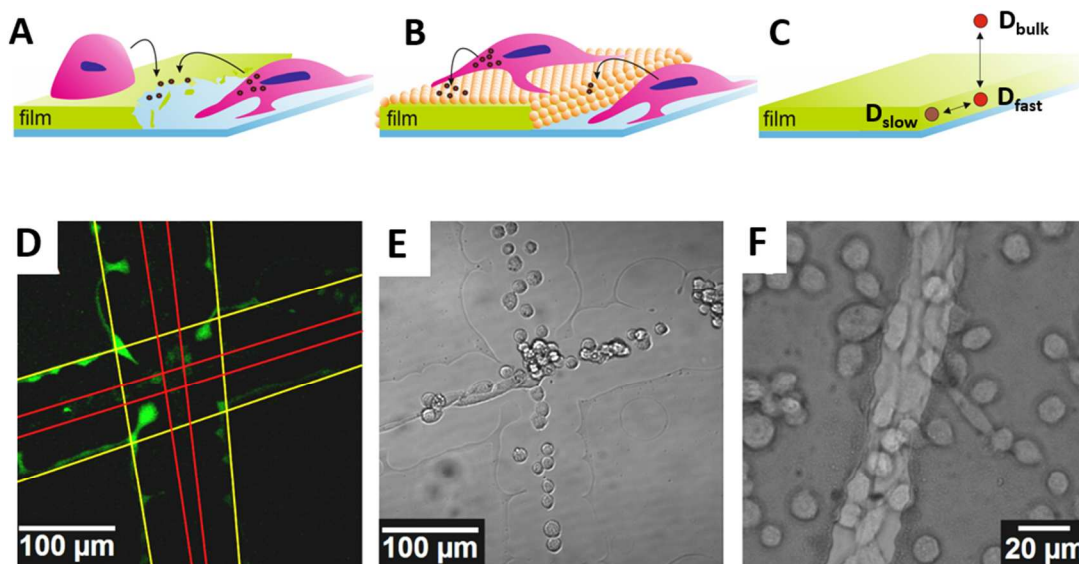
17 The extracellular matrix (ECM) provides not only a structural support for cellular growth, but  
18 also a biochemical milieu, which together define cell fate.<sup>1</sup> Artificial ECM is designed to mimic  
19 real ECM and to achieve cellular functions in laboratory designed materials similar as in nature.  
20 Artificial ECM consists of degradable supports made of natural or (semi)synthetic polymers  
21 which: i) recapitulate physical-chemical properties of real ECM, ii) host bioactive signaling  
22 molecules (e.g. hormones, cytokines, growth factors) to be presented to cells, and iii) possess  
23 tuned biodegradability.<sup>2-3</sup> The issues above are challenging for the fabrication of artificial ECM  
24 but are essential for successful applications in tissue engineering, diagnostics, and animal-free  
25 studies.  
26  
27  
28  
29  
30  
31  
32  
33  
34  
35  
36  
37

38 Introduced in the early nineties,<sup>4</sup> layer-by-layer deposition proofed to be extremely useful in  
39 the field of bio-functional coatings. It is powerful technique for the fabrication of polymer-based  
40 multilayer films with dimensions from nano to micro, adjusted composition, and tunable cellular  
41 response.<sup>5-11</sup> Control over cellular functions such as adhesion, differentiation, and  
42 proliferation,<sup>12-15</sup> along with reservoir properties for a variety of biomolecules such as proteins,  
43 growth factors, genes, and drugs<sup>7, 16-20</sup> makes these films an attractive platform for cell-based  
44 applications.  
45  
46  
47  
48  
49  
50  
51  
52  
53

54 Despite the evident biological potential to employ the multilayers to recapitulate ECM,<sup>3</sup> the  
55 options to tune multilayer biodegradability are mostly limited to multilayer chemical  
56  
57  
58  
59  
60

1  
2  
3 crosslinking<sup>13, 21-22</sup> that can significantly change multilayer properties. There is also a lack in  
4  
5 understanding the mechanism of biomolecule-multilayer interaction that obviously defines  
6  
7 biomolecule presentation/release from multilayers to cells and, as a result, cellular response.<sup>23-24</sup>  
8  
9

10 In this work a new approach for the design of artificial ECM with controlled biodegradation  
11 based on the coating of multilayers with gold nanoparticles (GNPs) is present. The multilayers  
12 were assembled from glycosaminoglycan hyaluronic acid (HA) and polyaminoacid poly-L-lysine  
13 (PLL). Molecular transport through the GNP-coated multilayers is investigated. The model  
14 protein lysozyme (Lys) has been loaded into multilayers as a mimic of ECM soluble signaling  
15 molecule. Protein mobility has been assessed by Fluorescence Recovery after Photobleaching  
16 (FRAP) to reveal protein availability to cellular receptors. The schematics in Figure 1A-C  
17 illustrates the multilayer biodegradation and the exchange of Lys in solution and in multilayers.  
18  
19  
20  
21  
22  
23  
24  
25  
26  
27  
28



48  
49  
50  
51  
52  
53  
54  
55  
56  
57  
58  
59  
60

**Figure 1.** Schematics of cellular interaction with (A) bare and (B) GNP-coated (HA/PLL)<sub>24</sub> multilayers. The coating protects the multilayer from degradation by the cells adhering on it. (C) illustrates exchange of Lys (red cycles) between bulk and the multilayers where fast and slow diffusive populations are present. (D) CLSM fluorescence and (E, F) transmission images of

1  
2  
3 L929 fibroblasts cells cultured for three days on (HA/PLL)<sub>24</sub> and on (F) GNP-coated (HA/PLL)<sub>24</sub>  
4  
5 multilayers ( $\gamma = 3$ ). Red and yellow lines in (D) represent scratch boundaries before and after cell  
6  
7 cultivation, respectively.  
8  
9

10  
11 Firstly, cellular interaction with the (HA/PLL)<sub>24</sub> multilayers has been assessed. The multilayers  
12  
13 have been scratched by a needle to form a visible scratched area of about 20  $\mu\text{m}$  (Figure S1).  
14  
15 This followed by seeding of L929 fibroblast cells which grow preferentially within the scratch  
16  
17 (Figure 1D-E) due to soft nature of bare multilayers.<sup>21, 25</sup> The scratch width has significantly  
18  
19 widened up to 100  $\mu\text{m}$  demonstrating the enzymatic degradation potential of cells. The  
20  
21 multilayers incubated without cells are stable, whereas those incubated with cells underwent  
22  
23 considerable degradation, most probably due to hydrolytic enzymes secreted by cells (Figure 1,  
24  
25 S1). Reduction of fluorescence in PLL-FITC containing multilayers is most likely caused by  
26  
27 biodegradation (Figure S1).  
28  
29  
30  
31

32  
33 Figure 1F shows a transmission image of the GNP-coated multilayers after 3 days of cell  
34  
35 culture. The amount of GNPs corresponds to three theoretical monolayers of compactly packed  
36  
37 spheres ( $\gamma = 3$ ). Improved cellular adhesion (Figure 1F and Figure S2) compared to uncoated  
38  
39 multilayers correlates well with our previous results showing that better adhesion of cells was  
40  
41 attributed to multilayer stiffening induced through the presence of nanoparticles on the  
42  
43 multilayer surface.<sup>26-27</sup> Hence, the coated multilayers become not only cell-adhesive but also  
44  
45 resistant to biodegradation, as indicated by a constant width of the scratch during and after  
46  
47 cellular growth (Figure 1F). One can assume that the coating acts as a barrier and prevents  
48  
49 diffusion of cell-expressed enzymes into the multilayers and, as a result, suppresses multilayer  
50  
51 biodegradation.  
52  
53  
54  
55  
56  
57  
58  
59  
60

1  
2  
3 To prove this assumption, transport of the molecules of different sizes and charges into the  
4 GNP-capped multilayers has been studied. A small dye 5(6)-carboxyfluorescein (376 Da, CF),  
5 large positively charged PLL-FITC (15-30 kDa), and dextrans-FITC of various molecular masses  
6 (10-500 kDa) have been employed as probes. The level of GNP coverage (GNPs covers only the  
7 multilayer surface) has been varied by adjusting the number of theoretical GNP monolayers ( $\gamma =$   
8 1.5 or 3).<sup>26</sup> The diffusion of CF into the film occurs almost instantaneously, regardless of  $\gamma$   
9 (Figure S3A). However, the situation is essentially different for larger PLL-FITC. While PLL-  
10 FITC saturates the bare films within 20-30 min, its diffusion is slowed down for the coated films  
11 ( $\gamma = 1.5$ ) and totally blocked if  $\gamma = 3$  (Figure 2A and Figure S3B). The fact that the diffusion of  
12 PLL-FITC is not significantly reduced for  $\gamma = 1.5$  compared to that at  $\gamma = 1.5$  may be related to  
13 defects in the GNP coating. The coating is not ideally homogeneous as proven by microscopy  
14 analysis. GNPs form clusters of several hundred nanometers and significant reinforcement of  
15 mechanical properties of the GNP coated (HA/PLL)<sub>24</sub> multilayers takes place at  $\gamma$  more than 1.5  
16 when the clusters are well interconnected.<sup>26</sup>

17  
18  
19  
20  
21  
22  
23  
24  
25  
26  
27  
28  
29  
30  
31  
32  
33  
34  
35  
36 One can assume that the GNP coating provides a kind of size-exclusion semipermeable barrier  
37 that does not possess diffusion limitations for small molecules. Diffusion of macromolecules is  
38 significantly reduced and depends on  $\gamma$ . However, molecular transport into the coated multilayers  
39 can not only be driven by the size of diffusing molecules but also by the interactions between the  
40 probe and multilayers. In the case of charged molecules (CF, PLL) electrostatics may play a  
41 significant role because of a large number of both positive and negative uncompensated charges  
42 in multilayers.<sup>23</sup> Negative charge on citric acid stabilized nanoparticles may thus also play a role.  
43  
44  
45  
46  
47  
48  
49  
50  
51

52  
53 Therefore, uncharged molecules - dextrans - of various molecular masses (10, 70, and 500  
54 kDa) have been employed to evaluate the impact of molecular mass to permeability. Figure 2B  
55  
56  
57  
58  
59  
60

shows that the cut-off of the uncoated films is between 70 and 500 kDa. Diffusion of 500 kDa dextran is fully hindered and 10 and 70 kDa dextrans can rather easily penetrate into the film, reaching saturation levels after 30 min of incubation (Figure 2B). A similar time is necessary to saturate the film with charged PLL (Figure 2A). This allows one to assume that the mesh size of the polymer network of the film plays the pivotal role in diffusion of macromolecules. In the case of the GNP-coated multilayers ( $\gamma = 3$ ) the dextrans do not diffuse into the films at all (Figure 2C). Systematic analysis of molecular diffusion through the GNP coating may allow adjusting the diffusion rate of a molecule of chose. Altogether, the coating can effectively suppress the degradation of the multilayers by preventing the diffusion of rather large enzymes such as hyaluronidase (Mw  $\sim$  54 kDa) and proteases (Mw are usually few tens of kDa). At the same time, transport of smaller protein-based biomolecules such as growth factors into/from the multilayers could still be possible and can also be adjusted by the  $\gamma$ .

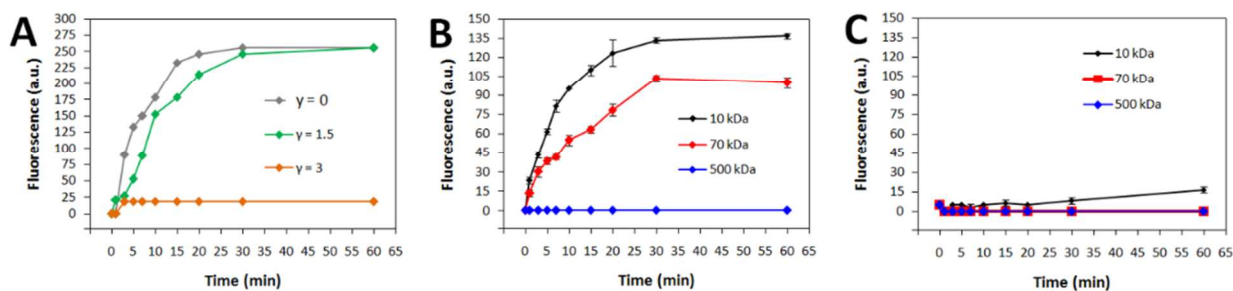


**Figure 2.** (A) Relative fluorescence of bare and GNP-coated (HA/PLL)<sub>24</sub> multilayers in the presence of PLL-FITC; the coating at  $\gamma=1.5$  or  $\gamma=3$ . (B) Relative fluorescence of the bare and (C) coated multilayers ( $\gamma = 3$ ) in the presence of 10, 70, and 500 kDa dextran-FITC.

The semipermeable nature and potential to adjust molecular transport into/from the multilayers make the coating attractive for the design of biomaterials with controlled degradability and controlled presentation/release of the loaded bio-molecules. The (HA/PLL)<sub>24</sub> multilayers can host

1  
2  
3 bio-macromolecules such as proteins which are rather mobile in the multilayers. Diffusion  
4 coefficient ( $D$ ) of proteins papain, lysozyme, and catalase were found to be about  $2-4 \mu\text{m}^2/\text{s}$ <sup>23</sup>  
5  
6 that shows the multilayers as good mimics of ECM in terms of mobility of proteins/growth  
7  
8 factors. The mechanism of protein loading/release into/from multilayers is still not clear showing  
9  
10 complex character of protein-multilayer interaction because of no systematic effect of protein  
11  
12 charge and size.<sup>23</sup>  
13  
14  
15

16  
17 For the reasons given above, the interaction of the model protein lysozyme with the  
18 multilayers has further been examined. Lys-FITC has been loaded into the multilayers, washed  
19  
20 out with Tris buffer and further with cell culture medium with systematic assessment of the  $D$  of  
21  
22 Lys and protein fluorescence in the multilayers.  $D$  of Lys in the multilayers has been evaluated  
23  
24 by FRAP according to the procedure described elsewhere, which is based on the analytical  
25  
26 solution of Fick's law of diffusion.<sup>23, 28-29</sup> The protein-loaded multilayers have been bleached  
27  
28 within a predefined area (marked with a yellow rectangle in Figure 3A) and the averaged 2D  
29  
30 fluorescence profile has been taken perpendicular to the bleached line. During the time course  
31  
32 the bleached and non-bleached Lys-FITC molecules exchange in the multilayers, resulting in the  
33  
34 widening of the fluorescence profile (profile width  $w$ ) and reduction of the depth of the profile  
35  
36 ( $A$ ) (Figure 3B and 3C). The intensity of fluorescence  $I(x,t)$  across the bleached region has been  
37  
38 approximated by the Gaussian function and is described by Equation 1:  
39  
40  
41  
42  
43  
44

$$I(x, t) = I_0 - A(t) \cdot \exp\left(-\frac{x^2}{2w^2}\right) \quad (\text{Equation 1})$$

45  
46 where  $I_0$  is the intensity of fluorescence before bleaching;  $A(t)$  is the depth of dip after time  $t$   
47  
48 following the bleaching;  $x$  is the spatial distance from the minimum of the dip and  $w$  describes  
49  
50 the half width of the Gaussian curve at the inflexion point.  
51  
52  
53  
54  
55  
56  
57  
58  
59  
60



1  
2  
3 High level of consistency of the experimental data fitted by the Equation 1 allows  $D$  to be  
4 determined reliably from the slope of linear regression of  $w^2$  plotted versus  $t$  (Figure 3D). The  
5 mean  $D$  of the protein loaded into the film has been found to be  $1.2 \pm 0.1 \mu\text{m}^2/\text{s}$  (in cell culture  
6 medium). Further two protein populations have been revealed in the multilayers (for details see  
7 Experimental part). The time evolution of the dip depth  $A$  was meant to test if a complete  
8 fluorescence recovery takes place, which would be indicative for a single protein diffusing  
9 population. Extrapolation of the initial kinetics of the changes of  $A$  indicates that  $A$  approaches a  
10 constant value (Figure 3E) which represents the fraction of protein molecules (about 10 % of all  
11 protein) that diffuse much slower compared to the main protein population in the multilayers.  
12 Thus, one can identify two populations of the protein molecules in the multilayers: Fast diffusing  
13 (major fraction, 90%,  $D_{\text{fast}}$ ) and slow diffusing proteins (minor fraction, 10%,  $D_{\text{slow}}$ ). Both  $D_{\text{fast}}$   
14 and  $D_{\text{slow}}$  contribute to the mean  $D$  measured with  $D_{\text{fast}} \gg D_{\text{slow}}$ . The slow diffusing fraction is  
15 approximated as immobile; diffusion slower than  $0.01 \mu\text{m}^2/\text{s}$  is undistinguishable from immobile  
16 behaviour because of spatiotemporal resolution of the experiment. Due to the small content of  
17 slow diffusing protein with  $D_{\text{slow}}$ , its contribution can be considered as minor, thus assuming that  
18  $D_{\text{fast}} \approx 1.0 \mu\text{m}^2/\text{s}$ . This value indicates rather fast protein diffusion and differs only by two orders  
19 of magnitude to protein diffusion in solution ( $D_{\text{bulk}}$ ) which is approximately  $100 \mu\text{m}^2/\text{s}$ ,  
20 according to Stokes-Einstein equation and reported literature data.<sup>23</sup> Figure 1C depicts exchange  
21 of Lys molecules between bulk and the film where fast and slow diffusive populations are  
22 present.

23  
24  
25 To understand if equilibrium between the diffusing populations is established, both the protein  
26 content in the film reflected by Lys-FITC fluorescence intensity and the content of immobile  
27 protein fraction have been considered during the protein loading and after sequential washing out  
28  
29  
30  
31  
32  
33  
34  
35  
36  
37  
38  
39  
40  
41  
42  
43  
44  
45  
46  
47  
48  
49  
50  
51  
52  
53  
54  
55  
56  
57  
58  
59  
60

with Tris-buffer and further with cell culture medium (Figure 3F). It is of note that cell culture medium does not affect Lys-FITC fluorescence (data not shown) meaning that the change in fluorescence indicates loss of protein washed out of the multilayers. After washing with buffer and finally with cell culture medium, the amount of protein in the multilayer film has been significantly reduced down to  $11 \pm 2\%$  compared to the initial protein content. At the same time, the content of the slow diffusing fraction is not enhanced and did not exceed 10% of the total protein (Figure 3F). This means that equilibrium is established between slow and fast protein fractions in the films within the time scale of tens of minutes (washing time).

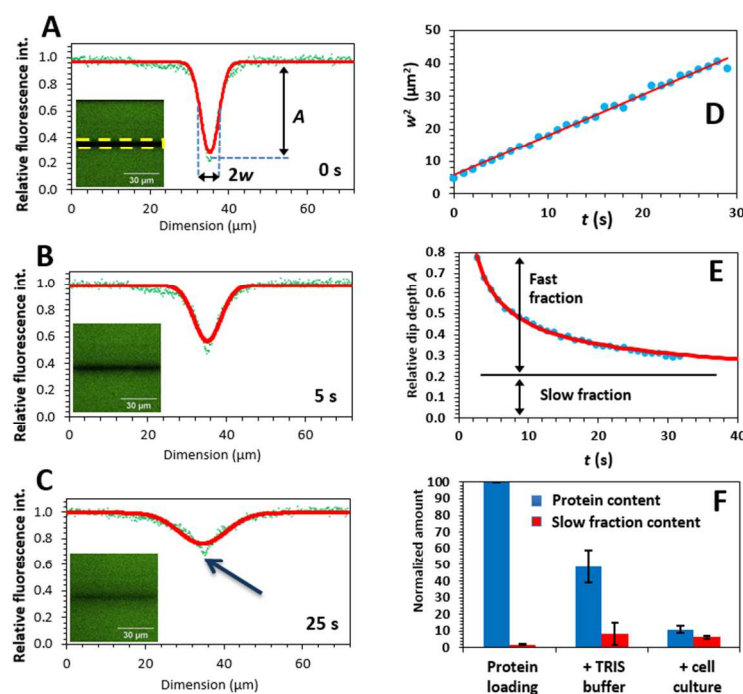


**Figure 3.** (A-C) - The recovery profiles at various time points (0, 5, and 25 s) after bleaching of  $(\text{HA}/\text{PLL})_{24}$  multilayers loaded with Lys-FITC (fluorescence images are as insets, the bleached area is marked by the dashed yellow rectangle). The experimental data are in green and the fitting curve in red; the fitting is performed using the Eq. 1. Gaussian width of the profiles ( $w$ ) and the relative dip depth ( $A$ ) have been determined as shown in (A). The blue arrow in (C) points to a dip in the recovery curve that indicates a protein fraction diffusing much slower than

1  
2  
3 the majority of protein molecules in the film. (D) -  $w^2$  versus recovery time  $t$  after bleaching, (E)  
4 - time dependence of relative dip depth  $A$  after bleaching plotted versus recovery time  $t$ , (F) -  
5 normalized fluorescence of multilayers loaded with Lys-FITC (in blue) and content of slow  
6 diffusing protein fraction (in red) after the protein loading followed by washing with TRIS and  
7 further with cell culture medium.  
8  
9

10  
11  
12  
13  
14  
15  
16 The presence of two protein populations in the film with significantly different mobility may  
17 be attributed either to i) the presence of two types of protein binding sites in the multilayers or ii)  
18 the formation of protein aggregates which are significantly larger than single protein molecules  
19 and thus diffuse much slower. The increase of the slow diffusing fraction with time during  
20 protein loading into the film<sup>30</sup> suggests that the slow diffusing fraction exists due to inter-protein  
21 interactions in the multilayers (protein aggregation). The presence of different protein binding  
22 sites would result in preferential protein binding to the site with stronger affinity and as a result  
23 reduction of the amount of slow diffusing proteins during the protein loading. The findings of  
24 this study stimulate further investigation, which we plan in the future in order to better  
25 understand the interactions between proteins and multilayers and tune multilayer biodegradation  
26 rate.  
27  
28  
29  
30  
31  
32  
33  
34  
35  
36  
37  
38  
39  
40  
41

42 In conclusion, the coating of biopolymer-based (HA/PLL)<sub>24</sub> multilayers with GNPs results in  
43 the formation of a size-exclusion semipermeable membrane on the multilayer surface with a cut-  
44 off tuned by GNP density. The GNP coating significantly improves cellular adhesion and protect  
45 the multilayers from biodegradation Analysis of protein (Lys) diffusion in the multilayers has  
46 revealed that the loaded protein molecules are present in two populations with high ( $D \approx 1.0$   
47  $\mu\text{m}^2/\text{s}$ ) and low ( $D_{\text{slow}} < 0.01 \mu\text{m}^2/\text{s}$ ) mobility. The populations are in equilibrium with each other  
48 and the fast diffusing population dominates, representing about 90% of the loaded protein. The  
49  
50  
51  
52  
53  
54  
55  
56  
57  
58  
59  
60

1  
2  
3 slow diffusing population is likely a result of protein aggregation. High mobility of the proteins  
4  
5 in the multilayers shows high promise to use the multilayers as hosts to present the loaded  
6  
7 bioactive molecules (e.g. growth factors, cytokines, hormones) to cell receptors. Finally, this  
8  
9 study demonstrates that GNP-coated (HA/PLL)<sub>24</sub> multilayers can potentially be exploited as  
10  
11 degradation-resistant drug delivery platforms suitable for cell culture and tissue engineering.  
12  
13  
14  
15  
16

17  
18 **Supporting Information** The supporting information includes experimental section, multilayers  
19  
20 stability tests, cellular adhesion to and kinetics of loading of CF and PLL-FITC into bare and  
21  
22 GNP-coated multilayers. This material is available free of charge via the Internet at  
23  
24 <http://pubs.acs.org>.  
25  
26

### 27 28 **Corresponding Author**

29  
30 \* Dr Dmitry V. Volodkin, School of Science and Technology, Nottingham Trent University,  
31  
32 Clifton Lane, Nottingham NG11 8NS, United Kingdom. E-mail: [dmitry.volodkin@ntu.ac.uk](mailto:dmitry.volodkin@ntu.ac.uk).  
33  
34  
35

### 36 37 **Author Contributions**

38  
39 The manuscript was written through contributions of all authors. All authors have given approval  
40  
41 to the final version of the manuscript. ‡Vladimir Z. Prokopović and Anna S. Vikulina contributed  
42  
43 equally to this work.  
44  
45

46  
47 **ACKNOWLEDGMENT** This work was supported by the Alexander von Humboldt Foundation  
48  
49 in the framework of the Sofja Kovalevskaja program and by DFG grant VO 1716/2-3.  
50  
51

### 52 53 **REFERENCES**

54  
55  
56  
57  
58  
59  
60

- 1  
2  
3 1. Lutolf, M. P.; Hubbell, J. A. Synthetic Biomaterials as Instructive Extracellular  
4 Microenvironments for Morphogenesis in Tissue Engineering. *Nat Biotech* 2005, 23 (1),  
5 47-55.  
6  
7
- 8  
9  
10 2. Kim, B.-S.; Park, I.-K.; Hoshihara, T.; Jiang, H.-L.; Choi, Y.-J.; Akaike, T.; Cho, C.-  
11 S. Design of Artificial Extracellular Matrices for Tissue Engineering. *Prog. Polym. Sci.*  
12 2011, 36 (2), 238-268.  
13  
14
- 15  
16  
17 3. Guillame-Gentil, O.; Semenov, O.; Roca, A. S.; Groth, T.; Zahn, R.; Voros, J.;  
18 Zenobi-Wong, M. Engineering the Extracellular Environment: Strategies for Building 2D  
19 and 3D Cellular Structures. *Adv. Mater.* 2010, 22 (48), 5443-5462.  
20  
21
- 22  
23  
24 4. Decher, G.; Hong, J.-D. Buildup of Ultrathin Multilayer Films by a Self-Assembly  
25 Process: I. Consecutive Adsorption of Anionic and Cationic Bipolar Amphiphiles.  
26  
27  
28  
29  
30  
31  
32  
33  
34  
35  
36  
37  
38  
39  
40  
41  
42  
43  
44  
45  
46  
47  
48  
49  
50  
51  
52  
53  
54  
55  
56  
57  
58  
59  
60
5. Gribova, V.; Auzely-Velty, R.; Picart, C. Polyelectrolyte Multilayer Assemblies on  
Materials Surfaces: From Cell Adhesion to Tissue Engineering. *Chem. Mat.* 2011, 24 (5),  
854-869.
6. Lavalle, P.; Voegel, J. C.; Vautier, D.; Senger, B.; Schaaf, P.; Ball, V. Dynamic  
Aspects of Films Prepared by a Sequential Deposition of Species: Perspectives for Smart  
and Responsive Materials. *Adv. Mater.* 2011, 23 (10), 1191-1221.
7. Pavlukhina, S.; Sukhishvili, S. Polymer Assemblies for Controlled Delivery of  
Bioactive Molecules from Surfaces. *Adv. Drug Deliv. Rev.* 2011, 63 (9), 822-836.
8. de Villiers, M. M.; Otto, D. P.; Strydom, S. J.; Lvov, Y. M. Introduction to  
Nanocoatings Produced by Layer-by-layer (LbL) Self-assembly. *Adv. Drug Deliv. Rev.*  
2011, 63 (9), 701-715.

- 1  
2  
3 9. Ariga, K.; Lvov, Y. M.; Kawakami, K.; Ji, Q. M.; Hill, J. P. Layer-by-Layer Self-  
4 assembled Shells for Drug Delivery. *Adv. Drug Deliv. Rev.* 2011, 63 (9), 762-771.  
5  
6
- 7  
8 10. Ariga, K.; Yamauchi, Y.; Rydzek, G.; Ji, Q. M.; Yonamine, Y.; Wu, K. C. W.;  
9 Hill, J. P. Layer-by-layer Nanoarchitectonics: Invention, Innovation, and Evolution.  
10  
11 *Chem. Lett.* 2014, 43 (1), 36-68.  
12  
13
- 14  
15 11. Gentile, P.; Carmagnola, I.; Nardo, T.; Chiono, V. Layer-by-layer Assembly for  
16  
17 Biomedical Applications in the Last Decade. *Nanotechnology* 2015, 26 (42).  
18  
19
- 20 12. Richert, L.; Lavalle, P.; Payan, E.; Shu, X. Z.; Prestwich, G. D.; Stoltz, J.-F.;  
21  
22 Schaaf, P.; Voegel, J.-C.; Picart, C. Layer by Layer Buildup of Polysaccharide Films:  
23  
24 Physical Chemistry and Cellular Adhesion Aspects. *Langmuir* 2004, 20, 448-458.  
25  
26
- 27 13. Boudou, T.; Crouzier, T.; Ren, K.; Blin, G.; Picart, C. Multiple Functionalities of  
28  
29 Polyelectrolyte Multilayer Films: New Biomedical Applications. *Adv. Mater.* 2010, 22  
30  
31 (4), 441-467.  
32  
33
- 34 14. Crouzier, T.; Fourel, L.; Boudou, T.; Albiges-Rizo, C.; Picart, C. Presentation of  
35  
36 BMP-2 from a Soft Biopolymeric Film Unveils its Activity on Cell Adhesion and  
37  
38 Migration. *Adv. Mater.* 2011, 23 (12), H111-H118.  
39  
40
- 41 15. Muzzio, N. E.; Pasquale, M. A.; Gregurec, D.; Diamanti, E.; Kosutic, M.;  
42  
43 Azzaroni, O.; Moya, S. E. Polyelectrolytes Multilayers to Modulate Cell Adhesion: A  
44  
45 Study of the Influence of Film Composition and Polyelectrolyte Interdigitation on the  
46  
47 Adhesion of the A549 Cell Line. *Macromol. Biosci.* 2016, 16 (4), 482-495.  
48  
49
- 50 16. Prokopović, V. Z.; Duschl, C.; Volodkin, D. V. Hyaluronic Acid/Poly-l-Lysine  
51  
52 Multilayers as Reservoirs for Storage and Release of Small Charged Molecules.  
53  
54 *Macromol. Biosci.* 2014, 15 (10), 1357-1363.  
55  
56  
57  
58  
59  
60

- 1  
2  
3  
4  
5  
6  
7  
8  
9  
10  
11  
12  
13  
14  
15  
16  
17  
18  
19  
20  
21  
22  
23  
24  
25  
26  
27  
28  
29  
30  
31  
32  
33  
34  
35  
36  
37  
38  
39  
40  
41  
42  
43  
44  
45  
46  
47  
48  
49  
50  
51  
52  
53  
54  
55  
56  
57  
58  
59  
60
17. Volodkin, D.; Skirtach, A.; Mohwald, H., LbL Films as Reservoirs for Bioactive Molecules. In *Bioactive Surfaces*, Borner, H. G.; Lutz, J. F., Eds. Springer-Verlag Berlin: Berlin, **2011**, pp 135-161.
  18. Jewell, C. M.; Lynn, D. M. Multilayered Polyelectrolyte Assemblies as Platforms for the Delivery of DNA and other Nucleic Acid-based Therapeutics. *Adv. Drug Deliv. Rev.* 2008, 60 (9), 979-999.
  19. Hirano, Y.; Mooney, D. J. Peptide and Protein Presenting Materials for Tissue Engineering. *Adv. Mater.* 2004, 16 (1), 17-25.
  20. Chuang, H. F.; Smith, R. C.; Hammond, P. T. Polyelectrolyte Multilayers for Tunable Release of Antibiotics. *Biomacromolecules* 2008, 9 (6), 1660-1668.
  21. Richert, L.; Boulmedais, F.; Lavalle, P.; Mutterer, J.; Ferreux, E.; Decher, G.; Schaaf, P.; Voegel, J.-C.; Picart, C. Improvement of Stability and Cell Adhesion Properties of Polyelectrolyte Multilayer Films by Chemical Cross-Linking. *Biomacromolecules* 2003, 5 (2), 284-294.
  22. Schneider, A.; Vodouhê, C.; Richert, L.; Francius, G.; Le Guen, E.; Schaaf, P.; Voegel, J.-C.; Frisch, B.; Picart, C. Multifunctional Polyelectrolyte Multilayer Films: Combining Mechanical Resistance, Biodegradability, and Bioactivity. *Biomacromolecules* 2007, 8, 139-145.
  23. Uhlig, K.; Madaboosi, N.; Schmidt, S.; Jager, M. S.; Rose, J.; Duschl, C.; Volodkin, D. V. 3d localization and Diffusion of Proteins in Polyelectrolyte Multilayers. *Soft Matter* 2012, 8 (47), 11786-11789.

- 1  
2  
3 24. Vogt, C.; Ball, V.; Mutterer, J.; Schaaf, P.; Voegel, J. C.; Senger, B.; Lavalle, P.  
4  
5 Mobility of Proteins in Highly Hydrated Polyelectrolyte Multilayer Films. *J. Phys. Chem.*  
6  
7 *B* 2012, 116 (17), 5269-5278.  
8  
9  
10 25. Üzüüm, C.; Hellweg, J.; Madaboosi, N.; Volodkin, D. V.; von Klitzing, R. Growth  
11  
12 Behaviour and Mechanical Properties of PLL/HA Multilayer Films Studied by AFM.  
13  
14 *Beilstein J. Nanotechnol.* 2012, 3, 778-788.  
15  
16  
17 26. Schmidt, S.; Madaboosi, N.; Uhlig, K.; Köhler, D.; Skirtach, A.; Duschl, C.;  
18  
19 Möhwald, H.; Volodkin, D. V. Control of Cell Adhesion by Mechanical Reinforcement of  
20  
21 Soft Polyelectrolyte Films with Nanoparticles. *Langmuir* 2012, 28 (18), 7249-7257.  
22  
23  
24 27. Prokopović, V. Z.; Duschl, C.; Volodkin, D. V. Hyaluronic Acid/Poly-L-lysine  
25  
26 Multilayers Coated with Gold Nanoparticles: Cellular Response and Permeability Study.  
27  
28 *Polymer. Adv. Tech.* 2014, (25), 1342-1348.  
29  
30  
31 28. Sustr, D.; Duschl, C.; Volodkin, D. A FRAP-based Evaluation of Protein Diffusion  
32  
33 in Polyelectrolyte Multilayers. *Eur. Polym. J.* 2015, 68, 665-670.  
34  
35  
36 29. Seiffert, S.; Oppermann, W. Systematic Evaluation of FRAP Experiments  
37  
38 Performed in a Confocal Laser Scanning Microscope. *J. Microsc.-Oxf.* 2005, 220, 20-30.  
39  
40  
41 30. Velk, N.; Uhlig, K.; Duschl, C.; Volodkin, D. Mobility of Lysozyme in Poly(L-  
42  
43 lysine)/Hyaluronic Acid Multilayer Films. *Colloids Surfaces B: Biointerfaces* 2016, 147,  
44  
45 343-350.  
46  
47  
48  
49  
50  
51  
52  
53  
54  
55  
56  
57  
58  
59  
60



## Table of Contents

